# MODELING OF LOSS OF TAIL ROTOR EFFECTIVENESS CONDUCTING TO UNANTICIPATED YAW

**Fabrice Cuzieux, Pierre-Marie Basset, André Desopper**
ONERA Centre of Salon de Provence
Base Aérienne 701 - Ecole de l'Air
13661 Salon Air - France
*fabrice.cuzieux@onera.fr ; Pierre-Marie.Basset@onera.fr ; andre.desopper@onera.fr*

***Keywords***: *LTE, Tail rotor VRS, Interaction, Yaw stability*

## Abstract

*Helicopters pilots are warned of the circumstances under which a Loss of Tail Rotor Effectiveness (LTE) may be encountered, especially thanks to the FAA advisory Circular 90-95 [1]. This critical phenomenon has been a contributing factor in several helicopter accidents. Also known as its consequence denomination: "Unanticipated Right Yaw" (URY) for counterclockwise, and "Unanticipated Left Yaw" (ULY) for clockwise main rotor direction of rotation, it can occur during flight operations at low airspeed and is the result of an alteration in some way of the airflow passing through a conventional tail rotor.*

*Three different aerodynamic conditions potentially inducing a LTE have been identified: main rotor disc vortex interference with the tail rotor, tail rotor vortex ring state and weathercock stability.*

*This paper aims to introduce simple flight mechanics modeling of these phenomena in the Helicopter Overall Simulation Tool code (HOST[1]). First goal of this study was to get a better understanding of the aerodynamic conditions that lead to LTE. Second goal was to reach real time simulation ability of such phenomena in order to offer a training capability.*

## 1 Introduction

In the early 80's, the US Army was losing two OH58 per month due to unanticipated right yaw (URY) [2]. At this time, a tail rotor stall was suspected. Don Bloom, test pilot, has demonstrated that a loss of efficiency was the origin of phenomenon.

LTE aerodynamic precursors are now well understood, and detailed in the FAA advisory Circular 90-95 [1]. In this circular are described also the corresponding behaviors a pilot must have under such circumstances in order first to identify LTE, and secondly how to react to expect a correct recovery of the yaw authority. The remaining questions are concerning the ability to capture the impact of design parameters that can explain why some helicopters are more sensitive to LTE? How can we evaluate the foot margin of a helicopter facing LTE? Can we train pilots?

The present paper will first focus on the three different aerodynamic conditions that can induce LTE. After, is presented the modeling of the different aerodynamic phenomena that can participate to a better simulation of a classical tail rotor aerodynamic environment within the HOST code. All these contributions are then evaluated in comparison with experimental result issued from the bibliography.

[1] *HOST : Helicopter Overall Simulation Tool is the EUROCOPTER Flight mechanics code.*

## 2 Aerodynamic conditions inducing a LTE

As previously said, the FAA advisory Circular 90-95 [1] well describes the aerodynamic conditions potentially inducing a LTE. Hereafter are discussed each of these conditions and the actual state of the art upon their modeling. Thanks to the internet and available accident reports, 61 accidents have been identified between April 1996 and June 2005 due to LTE.

Not all the helicopters have the same main rotor direction of rotation. This means that the induced torque has to be countered with a tail rotor thrust oriented in the corresponding direction. Due to this, LTE is inducing unanticipated right yaw (URY) in case of a counterclockwise main rotor direction of rotation [20] and an unanticipated left yaw (ULY) in case of a clockwise main rotor direction of rotation [19].

### 2.1 Weathercock stability

The first identified aerodynamic condition potentially inducing a LTE is commonly called weathercock stability. It corresponds to tailwinds within a region from 120° to 240° that will tend to weathervane the nose of the aircraft into the relative wind (Fig. 1). This is essentially due to the force exerted by the wind on the fuselage and vertical fin.

If the helicopter enters such a relative rear wind condition, it will make a slow uncommanded turn either to the right or left, depending on the exact wind direction, unless a resisting pedal input is made. If the pilot allows a yaw rate to develop, because inattentive for some reason, it may increase. If this happens in the opposite direction of the main rotor rotation, the pedal margin can quickly become insufficient to counteract the yaw.

### 2.2 Tail Rotor Vortex Ring State

It has been well documented that a helicopter tail rotor can enter a vortex ring state (VRS) [3],[4]. During sideward flight or during a hover turn over a spot, a crosswind will oppose the tail rotor induced airflow.

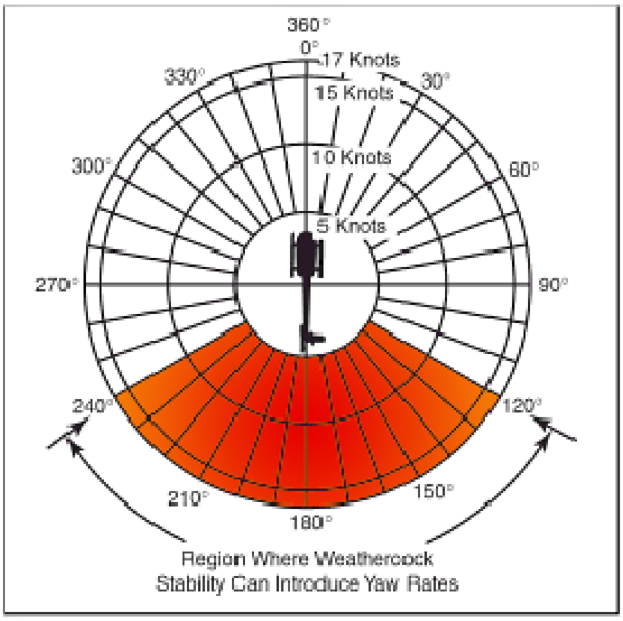


Fig. 1: Weathercock stability region

As for a main rotor in vertical descent, this can cause the VRS. Consequently, the tail rotor will experience thrust variations which may result in yaw deviations which require a potentially high pedal activity as illustrated in Fig. 2.

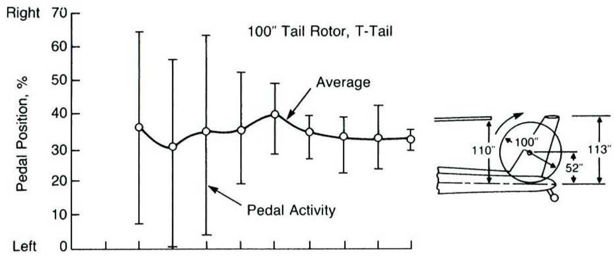


Fig. 2 : Pedal Activity in Left Sideward Flight of Hughes AH-64. [5]

More than thrust variation, VRS also results in a thrust drop. In [6], Blake and .al. have clearly identified this phenomenon in the case of an OH-58A, see Fig. 3.

As a result, if a tail rotor enters a VRS, the loss of thrust will induce a yaw rate that can accelerate dramatically.

Here again the main rotor direction of rotation and the corresponding tail rotor thrust orientation will influence the VRS relative wind region definition as illustrated in Fig. 4, which correspond to an adaptation of [1].

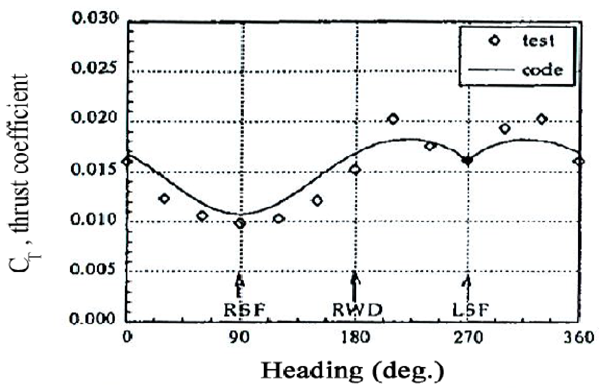


Fig. 3 : OH-58 tail rotor thrust coefficient variation with heading (45kts, collective=19°), issued from [4] as a reproduction of [6].

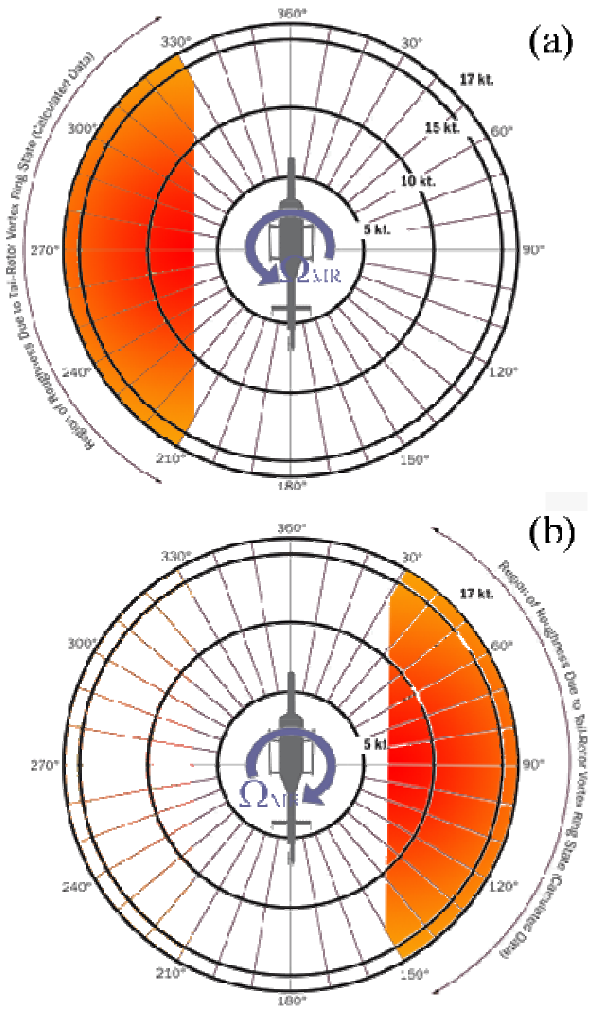


Fig. 4 : Region of roughness due to Tail rotor VRS, (a) for a counterclockwise main rotor direction of rotation, (b) for a clockwise main rotor direction of rotation

As documented by Prouty in [3], parameters, other than the relative wind, can strongly influence the VRS sensitivity of a tail rotor. First of all is the main rotor interference. The distance and relative position of the main and tail rotor can originate a more or less stronger influence and will be also discussed in the next section. Moreover it appears that the direction of rotation of the tail rotor can induce a dramatic difference in the pedal position in sideward flight. Fig. 5 issued from [7] illustrates this influence. Rotation with the bottom blade going aft is suspected to entrain the tip vortex of the main rotor, causing a premature VRS condition at the tail rotor.

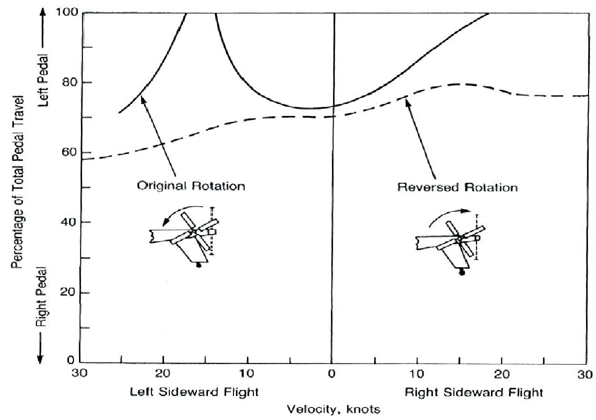


Fig. 5 : Typical Pedal Requirement for AH-56A in sideward flight for each tail rotor direction[7]

The last important factor influencing tail rotor VRS is mainly called the fin blockage. It corresponds to the interaction between the tail rotor and the vertical fin. Of course this interaction is reciprocal. Due to the relative position and dimension of the two, an adverse fin force is generated from the tail rotor induced velocity [4]. Also, a tail rotor thrust variation is to be considered. This thrust modification will impact the wind velocity value that will induce a tail rotor VRS.

Three main parameters are so to be considered here:

- *The Fin and tail rotor configuration, tractor or pusher (see* Fig. 6*)*
- *The distance between the two* [7].
- *The blockage ratio : S/A (see* Fig. 7*)*

As a conclusion, modelling of the tail rotor VRS influence over yaw stability, not only supposes a correct modelling of the tail rotor under VRS, but also the modelling of the interaction it has with the vertical fin.

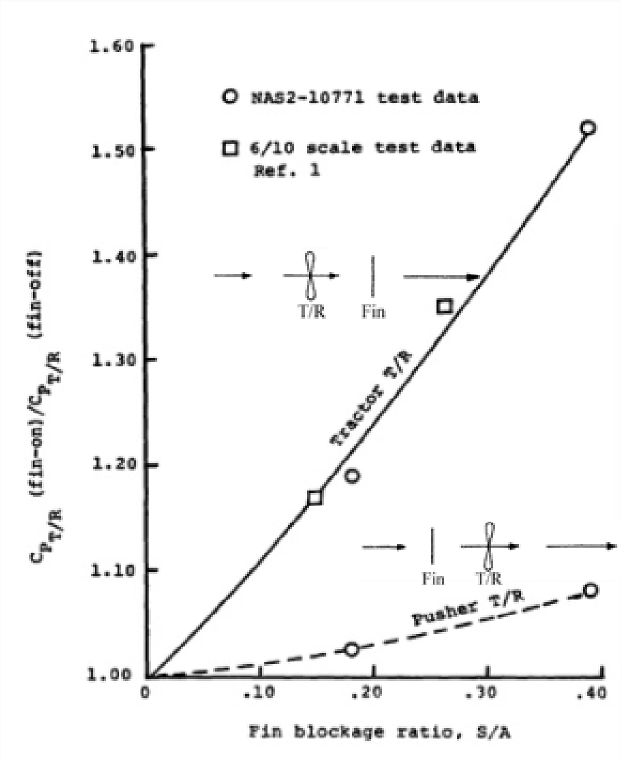


Fig. 6 : Tractor and Pusher configuration [8]

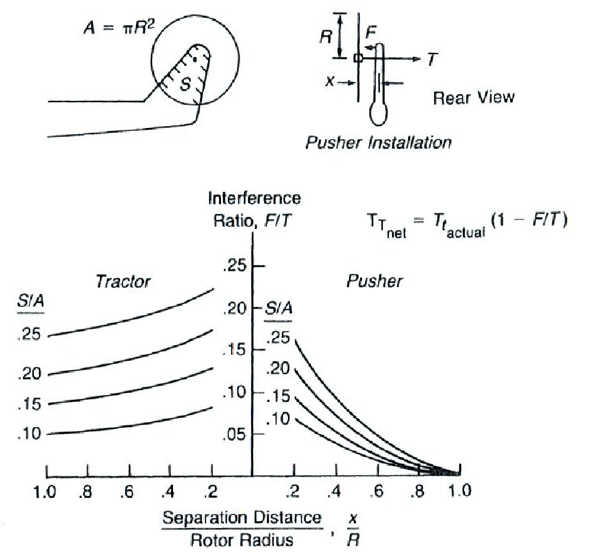


Fig. 7 : Tail Rotor-Fin Thrust Interference Ratio in Hover [5]

## 2.3 Main Rotor disc vortices / Tail Rotor Interaction

Last but not least is the interaction between the main rotor and the tail rotor. Of course, the momentum flow of the main rotor, especially in forward flight, has an influence on the tail rotor [7], and as already said its trailing vortices can influence strongly the tail rotor thrust. But, as described in the FAA advisory Circular 90-95 [1], a more dramatic influence of the main rotor can be encountered in quartering flight conditions. Many studies of the main rotor wake in quartering flight have highlighted the so called main rotor disc edge vortices strong influence on the tail rotor thrust [10],[11],[12].

In [13], Ellin well describes how the trailing vortices of the main rotor blades will aggregate in two contra-rotating macro-vortices under certain velocity conditions. This phenomenon is called the wake roll-up and can be illustrated by Fig. 8.

Fig. 8 : Main rotor disc Vortex illustration.

When passing through or near the tail rotor, such a vortex can influence strongly the inflow conditions. The extremely turbulent environment resulting from this interaction can induce tail rotor thrust variations because of angle of attack quick modifications. Both of the main rotor disc vortices can interact with the tail rotor depending on relative wind azimuth. Yet, as for the previous LTE aerodynamic conditions, the main rotor torque direction and so the resulting foot margin in left or right flight will influence the severity of the LTE. Fig. 9 illustrates the relative wind direction potentially inducing LTE due to main rotor disc vortex.

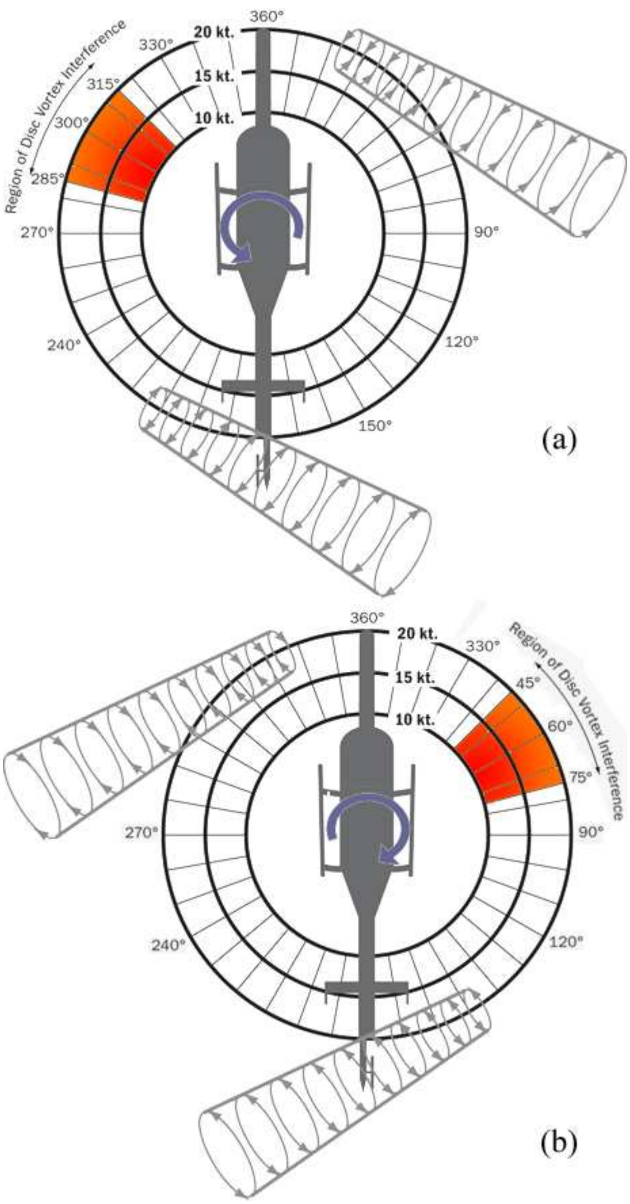


Fig. 9 : Region of main rotor disc vortex interference, (a) for a counterclockwise main rotor direction of rotation, (b) for a clockwise main rotor direction of rotation

## 3 Modeling of LTE

In order to simulate LTE, the following new modeling or adaptation have been studied by ONERA after a status on the available models keeping in mind the real time constrains.

A new modeling of the interaction between the tail rotor and the vertical fin will be introduced. Vortex ring state modeling is already present in the code, but previously developed for the main rotor. VRS simulation, will be discussed in the scope of the tail rotor VRS evaluation. Finally, a modeling of the main rotor disc vortex wake and its interaction with the tail rotor will be presented.

### 3.1 State of the art and the HOST code

#### *3.1.1 Weathercock stability*

Of course weathercock stability was already suitable in the HOST code. Thus wind influence over the vertical fin is achievable. However interaction between tail rotor and vertical fin influences the aerodynamic conditions under which operate the vertical fin. Therefore a comprehensive tail rotor/fin model is required for capturing their reciprocal aerodynamic influences.

Srinivas & al. [4] have provided an empirical modeling of such an interaction between the tail rotor and the fin. This can compute the adverse fin force as a function of wind speed, heading, tail rotor thrust and blockage ratio.

In R. Prouty's book [5] is also available an empirical evaluation of the interaction but only for hover condition. Fig. 7 resumes the experimental results used as an abacus. As one can see, here is taken into account for the Tail Rotor installation : Pusher/Tractor, the separation with vertical fin *x* and the blockage ratio *S/A*. Fig. 7 could be applied for evaluating the additive force correction on the fin as in the actual HOST modeling.

#### *3.1.2 Tail rotor vortex ring state*

The VRS has already been well modeled for a helicopter main rotor. "CFD model" [14] and more recently "Time marching unsteady wake model" [15] have proven their ability to represent such a state of the rotor wake. But, all these models are far from real time performance. Therefore, analytical model have been proposed in the past, like the empirical one available in W. Johnson's book [16]. At ONERA, another analytical model [17] has been established, based on Dauphin helicopter flight test data. These models aim to improve the induced velocity caluclation in VRS enabling to render the vertical speed drop and the insensitivity of the helicopter to collective pitch variations (power-settling) in such conditions.

In [4], V. Srinivas and al. have used W. Johnson's modeling for an OH-58 tail rotor and obtained good agreements with Blake and al. [6] experiments as illustrated in Fig. 3.

#### *3.1.2 Main Rotor disc vortex / Tail rotor interaction*

Due to its strong acoustic resultant, interaction between main rotor and tail rotor is well documented. But, for performance purpose and more precisely for quartering flight conditions, when the main rotor disc vortices form, there are few modeling investigation. The European collaborative project HELIFLOW [10],[11] was one of those. During Task 2 "Quartering Flight" of this project, multiple partners have used modeling tools including CAMRADII, VSAERO with more or less good agreements with experiments, see Fig. 10.

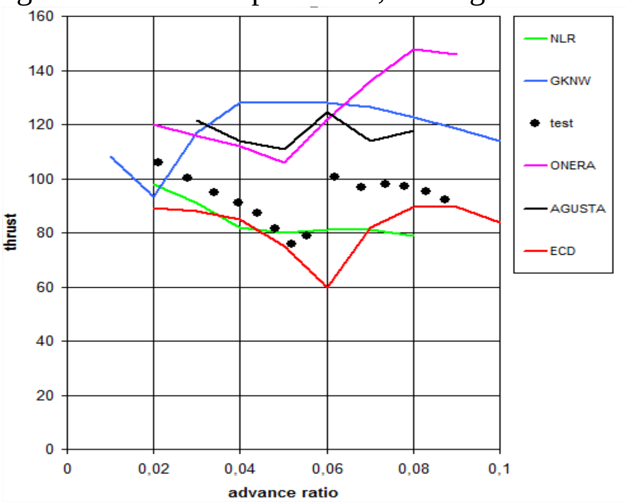


Fig. 10 : Tail rotor thrust for a range of advance ratio, low tail rotor TBA at 60° azimuth.

ONERA used at this time a simplified model of the induced normal and rotational velocities due to one main rotor disk edge vortex interacting with the tail rotor. This modeling was compliant with real time simulation and so will be detailed hereafter in an enhanced version implemented by ONERA in the HOST code.

### 3.2 Introduced modeling

In this part are discussed the models introduced in the HOST code in order to improve the code ability to reproduce the main aerodynamic conditions that can trigger LTE. These models catch main aerodynamic parameters as well as main relevant design parameters.

#### *3.2.1 Tail Rotor / Vertical Fin Interactions*

The main goal here was to provide a modeling of the influence of the tail rotor over the vertical fin relying on physical parameters explicitly. As mentioned, the actual modeling, which is based on the assumption of an adverse fin force proportional to the tail rotor thrust, can be used in conjunction with Fig. 7 as an abacus.

However, another modeling has been tested in the case of pusher configuration. Originally based on details given in [7] which stands for the computation of the tail rotor induced velocity in the plane of the fin in order to calculate the corresponding fin drag force, this approach had to be tested as the aerodynamic forces of the fin computation were only relying upon the relative wind. Thus a simple way to compute the fin adverse force is to correct this relative wind by taking into account the tail rotor induced velocity contribution. Thanks to tail rotor modeling, the induced velocity in its plane is already available. In order to get the induced velocity in the plane of the vertical fin an estimation of the tail rotor upstream flow is derived from a vortex ring with a radius corresponding to the tail rotor one. This allows taking into account for the tail rotor / finning relative distance '$D_{RD}$'. Then, to reproduce the influence of the fin blockage ratio, a fin aspired ratio $\%_{SD/SR}$ coefficient has been introduced as illustrated in Fig. 11. The relative wind correction is then defined as follow:

$$\Delta Vy_{DER} = V_{iTR} \cdot \%_{SD/SR} \cdot \sqrt{\cos\left(\tan^{-1}\left(\frac{D_{RD}}{R_{TR}}\right)\right)^3} \quad (1)$$

This modeling has then been superimposed with the OH-58 experiments available in [4] (see Fig. 11) with the tail rotor VRS modeling activated discussed in 3.2.2.

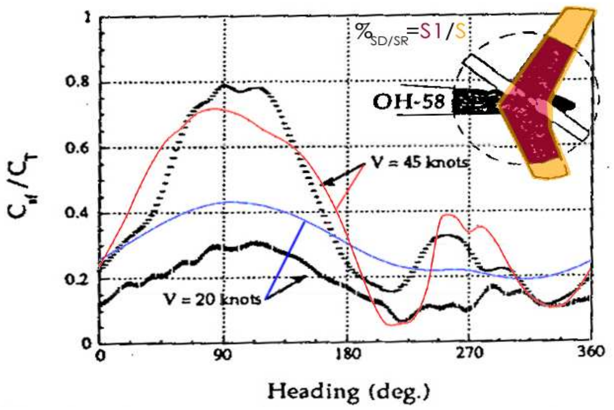


Fig. 11 : Fin Aspired Ratio definition

### 3.2.2 *Tail rotor vortex ring state*

For tail rotor VRS, it has been decided to use the actual vertical descent induced velocity modeling developed for the main rotor [17], and already available in the HOST code. This modeling corresponds to an extended momentum theory with a corrective coefficient introduced for taking the different losses into account [18]. This modeling is not far from the one proposed in [16] and used by Srinivas and al. in [4] for an OH-58 tail rotor (see Fig. 3).

An OH-58 isolated rotor has been reproduced in the HOST code in order to compare results with experiments available. Fig. 12 and Fig. 13 illustrate a good agreement between experiments and HOST VRS modeling results. Nevertheless, an artifact exist at 270° of heading which is due to the ??? of the mean induced velocity in the VRS region with respect to the velocity normal to the rotor disk in comparison with its dependency upon the edgewise velocity. Fig. 14 illustrates the behavior of the induced velocity around this region.

### 3.2.3 *Main Rotor disc vortex / Tail rotor interaction*

As already mentioned, a modeling of the main rotor disc vortex / tail rotor interaction has already been tested in HOST [10], but for HELIFLOW quartering flight conditions only.

In the present paper a more detailed version of this modeling is developed in order to be able to compute the interaction for every relative wind azimuths. Hereafter are described the main steps of the computational method.

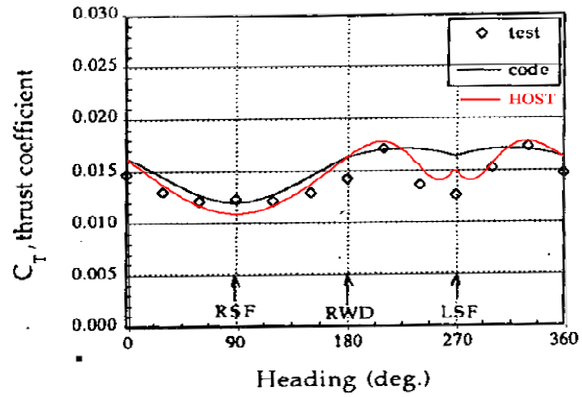


Fig. 12 : OH-58 Tail rotor thrust coefficient variation with heading (35kts, collective=19°)

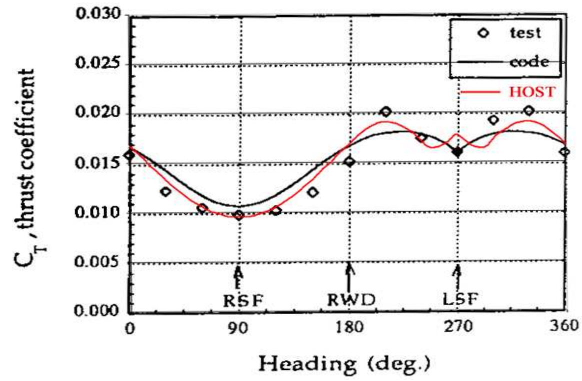


Fig. 13 : OH-58 Tail rotor thrust coefficient variation with heading (45kts, collective=19°)

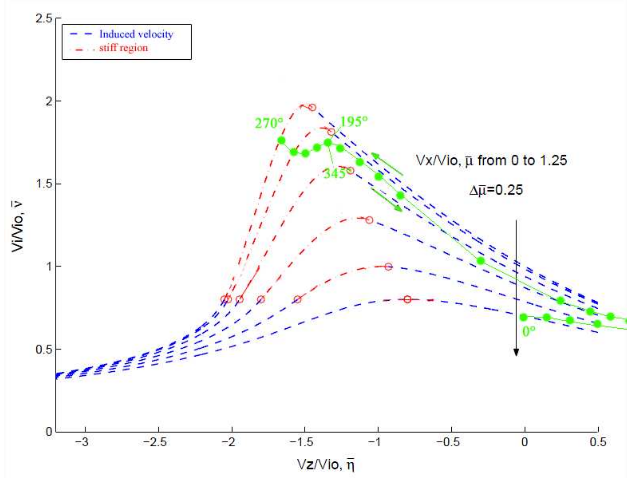


Fig. 14 : Induced velocity artifact illustration.

- Main rotor disc vortex wake geometry

Based on experimental observations [9], one can see that the main rotor wake can roll up into two disc edge vortices at low to intermediate flying speeds (≥35 knots).

These two vortices are not far from two rectilinear semi infinite vortices as supposed in the present modeling. Moreover, the rotor wake contracts asymptotically as illustrated in Fig. 15.

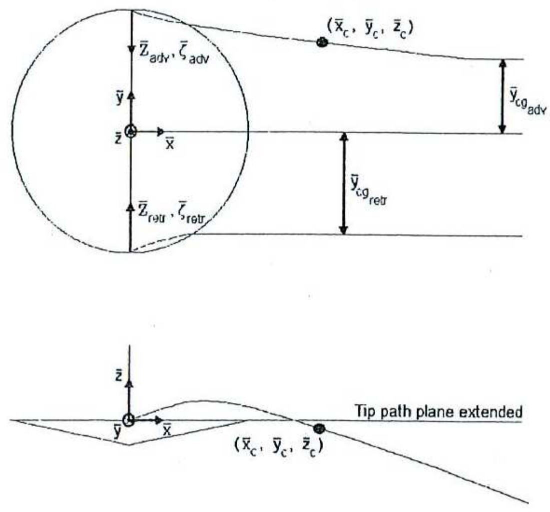

Fig. 15 : Scheme of the main rotor disc vortices issued from [9]

No difference between the advancing and retreating side is considered here. So the contraction is adjusted through an empirical correction factor $K_{CON}$ corresponding to the ratio of the asymptotic radius over the rotor radius. This contraction factor is usually between π/4 and 1.0 [9].

In order to stay coherent with the assumption of symmetric vortices, their strength are considered as the zero order term of J.P. Roos modeling [9], see equation (2).

$$\Gamma_{RP} \approx \mathrm{K}_{\mathrm{INT}} \cdot \frac{\pi}{2} \cdot \frac{2T}{\rho \Omega R_{MR}^2 \left(1 - \frac{3}{2}\mu^2\right)} \quad (2)$$

Again, a correction factor $K_{INT}$ is introduced to allow a better matching of the results when experiments are available.

Still based on J.P. Roos observations, the wake skew angle is partially induced by the mean rotor induced velocity and partially due to auto induction of the wake vortex sheet on itself. Considering these two parameters, a mean velocity in the wake $V_{IMwake}$ is computed as the balance between the mean induced velocity in the main rotor plane $V_{IMRP}$ and the induced airspeed by one semi-infinite vortex on the other, with a correction factor $K_{VIW}$.

$$V_{IMwake} = \mathrm{K}_{\mathrm{VIW}} \left( \frac{2\Gamma_{RP}}{4\pi . \mathrm{K}_{\mathrm{CON}} . R_{RP}} + V_{IMRP} \right) \Big/ 2 \quad (3)$$

Thanks to the previous equations and parameters, the full geometry of the rotor disc vortex approximation is available.

- Deriving the induced velocity

For being compliant with real time objectives, an analytical tail rotor modeling is usually applied for complete rotorcraft simulations. Typically this kind of modeling involves a computation of the rotor relative wind conditions at its center. In the HOST code it is possible to use a six component relative wind conditions ($\boldsymbol{U_{eq}}$, $\boldsymbol{V_{eq}}$, $\boldsymbol{W_{eq}}$, $\boldsymbol{\Omega_{Xeq}}$, $\boldsymbol{\Omega_{Yeq}}$, $\boldsymbol{\Omega_{Zeq}}$). The first three components correspond to the translational velocities and the three last ones to the rotational velocities around each axis.

Using Biot and Savart induction law it is possible to compute the induced velocities due to the main rotor disc vortices everywhere in space.

$$Vi = \frac{\Gamma\left(1 + \sin\left(\phi_{SILPT0}\right)\right)}{4\pi D_{RA0T0}} \quad (4)$$

As usually in vortex computation methods a viscous radius (VR) is defined in order to prevent from infinite velocities. Linear approximation is used for distance lower than VR. Moreover, an additional correction factor $K_{VR}$ is also introduced.

$$\mathrm{VR} = \mathrm{K}_{\mathrm{VR}} . \frac{2\mathrm{R}_{\mathrm{RP}}}{30} \quad (5)$$

These equations only give the ability to compute the three axial velocity components at the point considered. In order to compute at the center of the tail rotor (analytical model) the six components velocity vector, a method has been implemented.

$2^n$ points equally positioned all around the tail rotor at 3/4 of the radius are considered. At each point, the disc vortices induced velocity components ($\boldsymbol{U(\psi_p)}$, $\boldsymbol{V(\psi_p)}$, $\boldsymbol{W(\psi_p)}$) are evaluated, $\boldsymbol{\psi_p}$ standing for the blade azimuth in the rotor frame. With respect to the HOST conventions, these three components can be approximated at each point with the six components velocity vector as follow :

$$u(\psi_p) = u_{eq} + r\Omega_{Zeq}\sin\left(\psi_p + \frac{\pi}{2}\right)$$
$$v(\psi_p) = v_{eq} \pm r\Omega_{Zeq}\cos\left(\psi_p + \frac{\pi}{2}\right)$$
$$w(\psi_p) = w_{eq} - r\Omega_{Xeq}\sin\left(\psi_p + \frac{\pi}{2}\right) \mp .r\Omega_{Yeq}\cos\left(\psi_p + \frac{\pi}{2}\right) \quad (6)$$

The sign ± depends on the tail rotor direction of rotation with respect to the HOST conventions.

Thanks to the equi-repartition of the $2^n$ points (*nbpt*) and after some simplifications the following six components definition comes :

$$u_{eq} = \sum_{p=1}^{nbpt} \frac{u(\psi_p)}{nbpt}$$
$$v_{eq} = \sum_{p=1}^{nbpt} \frac{v(\psi_p)}{nbpt}$$
$$\Omega_{zeq} = \sum_{p=1}^{nbpt}\left(\frac{u(\psi_p)}{r.\sin(\psi_p+\frac{\pi}{2})} \pm \frac{v(\psi_p)}{r.\cos(\psi_p+\frac{\pi}{2})}\right) \Big/ (2.nbpt-4)$$
$$\forall p / \sin(\psi_p+\frac{\pi}{2}) \neq 0 \,\&\, \cos(\psi_p+\frac{\pi}{2}) \neq 0 \quad (7)$$

$$w_{eq} = \sum_{p=1}^{nbpt}\left(\frac{w(\psi_p)}{nbpt}\right)$$
$$\Omega_{xeq} = \sum_{p=1}^{nbpt}\left(\frac{w(\psi_p)}{r.\sin(\psi_p+\frac{\pi}{2})}\right) \Big/ (nbpt-2) \quad ,\forall p / \sin(\psi_p+\frac{\pi}{2}) \neq 0$$
$$\Omega_{yeq} = \sum_{p=1}^{nbpt}\left(\frac{\pm w(\psi_p)}{r.\cos(\psi_p+\frac{\pi}{2})}\right) \Big/ (nbpt-2) \quad ,\forall p / \cos(\psi_p+\frac{\pi}{2}) \neq 0 \quad (8)$$

In order to validate this new modeling, HELIFLOW experiments [11] have been used. Three significant configurations have been compared:

1. LOW, TBA : the tail rotor centre was at the same vertical position as the main rotor plane, with tail rotor direction of rotation Top Blade Aftward
2. LOW, TBF : the tail rotor centre was at the same vertical position as the main rotor plane, with tail rotor direction of rotation Top Blade Forward
3. HIGH, TBA : the tail rotor centre was higher than the vertical position of the main rotor plane, with tail rotor direction of rotation Top Blade Aftward

First, a comparison of the isolated tail rotor configurations TBF and TBA between experiments and HOST has been performed. Some parameters of the analytical rotor modeling have been tuned in order to better match the experiments. Then comparisons with tail rotor interacting with main rotor disc vortex have been computed without and with use of the different correction factors. Fig. 16, Fig. 17 and Fig. 18 highlight the results obtained compared to the experiments.

As one can see, results with no correction indicate that the model is perfectible but that it captures the main influencing parameters in a good way. To better match the experiments, the correction factors have been used in the following range :

$$0.65 \le K_{VR} \le 0.85$$
$$0.5 \le K_{VIW} \le 1.15$$
$$0.96 \le K_{CON} \le 0.98$$
$$1.05 \le K_{INT} \le 1.5$$

This range of use can be analyzed as follow:

- $K_{VR}$

The Viscous ray has been used to adjust the maximum intensity region. These experiments seem to indicate an over estimation of the VR in equation (5)

- $K_{VIW}$

This coefficient was used to get a better phasing of the modeling answer with respect to the experiments.

- $K_{CON}$

Even if this coefficient allows some amplitude corrections it has been mainly used in coherence with experimental observation made in HELIFLOW experiments [11].

- $K_{INT}$

This coefficient allows an amplitude correction over all the advancing ratio range. The values used seem to indicate a quite good uncorrected evaluation in the TBA configuration while the TBF needs a relative inflation of this parameter. This may be coherent to the conclusion of Prouty [5] in sideward flight. It is to say that in TBF configuration, the direction of rotation is the same as the incoming main rotor disc vortex orientation. This may accentuate the mutual interaction.

Next step would be to implement a higher order modeling of the vortex as done by J.P.Roos in [9] then allowing differentiating the disc vortex issued from the advancing blade side of the rotor from the retreating side. Such a modeling would also be able to provide a contraction factor computation instead of the actual coefficient $K_{CON}$.

Another approach which maybe still compliant with realtime simulation, consists in using the multi-vortex-rings model presented for example in [21] for a better modeling of the main rotor wake. For the calculation of the effect on the tail rotor, applying the same original method for the tail rotor analytical model provides the same good capture of the tail rotor thrust drop. The use of a tail rotor blade element model would be a next step, yet requiring more computational time.

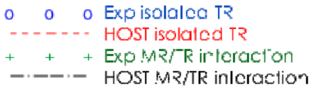


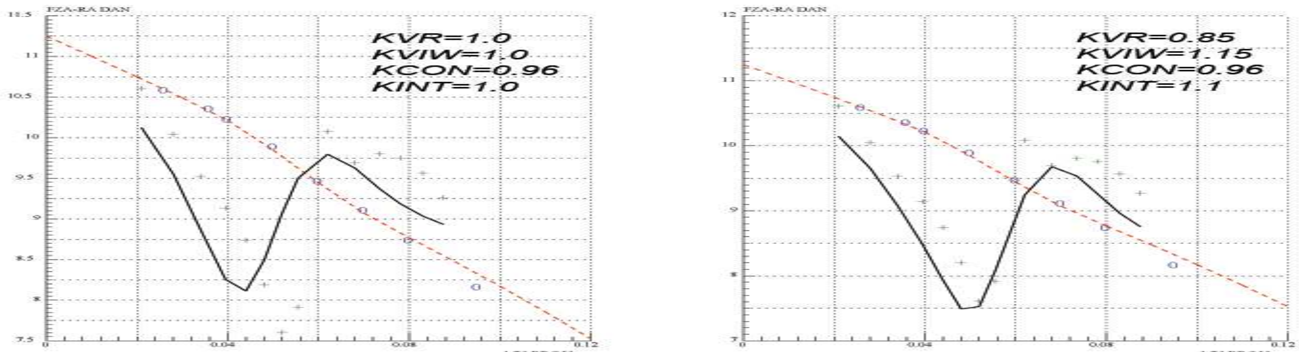


Fig. 16 : Comparison of tail rotor thrust between HOST results and experiment issued from HELIFLOW "Low Top Blade Aftward" configuration

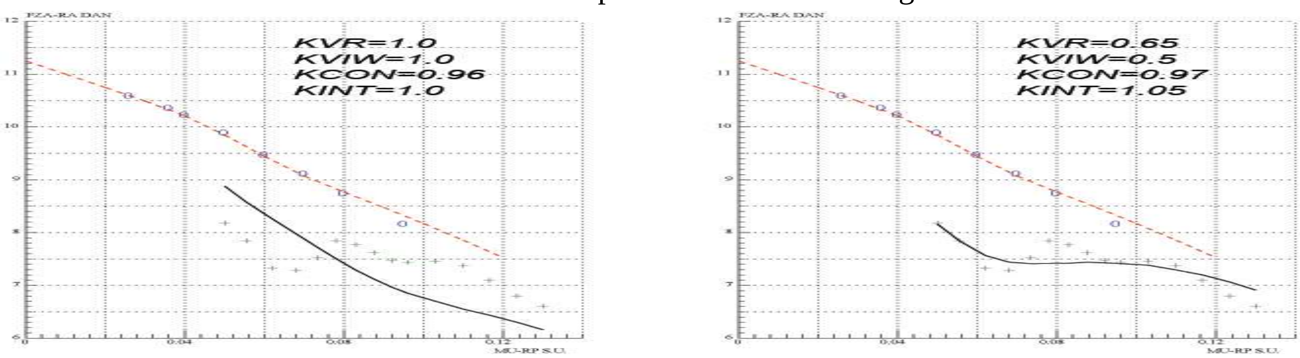


Fig. 17 : Comparison of tail rotor thrust between HOST results and experiment issued from HELIFLOW "High Top Blade Aftward" configuration

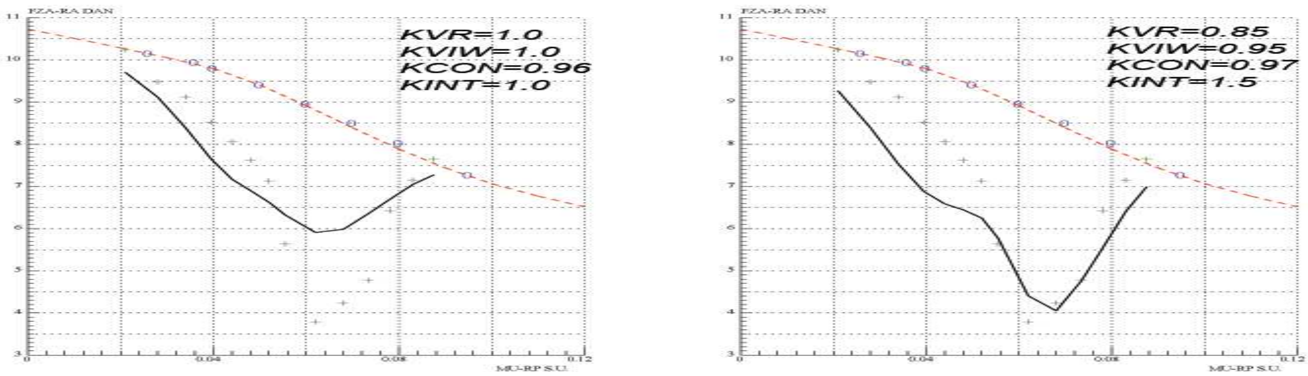


Fig. 18 : Comparison of tail rotor thrust between HOST results and experiment issued from HELIFLOW "Low Top Blade Forward" configuration

## 4 Conclusions

The present paper has introduced an overview of the aerodynamic conditions that can induce a Loss of Tail rotor Effectiveness regarding the main influencing design parameters. Models of these conditions including the most relevant design parameters influences have been proposed and included in the HOST code. Their agreements with available experimental results highlight their ability to capture most of the effects. Moreover, the relative simplicity retained all along the development of these models ensures real time compliance. Therefore, simulation with pilot in the loop can now be performed including the LTE risk.

## References


[1] Federal Aviation Administration: "*Unanticipated right yaw in Helicopters*", Advisory circular 90-95, issued on 12/26/95.

[2] Dan Megna: "LTE - the origine of loss of tail rotor effectiveness", Vertical flight magazine February-March 2005.

[3] Raymond W. Prouty, Helicopter Performance, Stability, and Control, Krieger Pub., 2002

[4] V. Srinivas, I. Chopra, D. Haas, K. McCool : « Prediction of Yaw Control Effectiveness and Tail Rotor Loads », 19th European Rotorcraft Forum, Cernobio (Como), Italy, Spet. 14-16 1993.

[5] Raymond W. Prouty, Development of the Empennage Configuration of the YAH-64 Advanced Attack Helicopter, USAAVRADCOM TR-82-D-22, 1983.

[6] Blake, Bruce; Hodder, David St. J.; and Hanker, Edward J., Jr.: Wind Tunnel Investigation Into the Directional Control Characteristics of an OH-58A Helicopter. USAAVRADCOM TR-83-D-18, U.S. Army, June 1984.

[7] Wiesner, W., and Kobler, G. "*Tail Rotor Design Guide*." USAAMRDL *TR 73-99*. January *1974*

[8] Menger, R. P.; Wood, T. L.; Brieger, J. T., Effects of aerodynamic interaction between main and tail rotors on helicopter hover performance and noise, 1983, NASA-CR-166477.

[9] J.P. Roos : "An analytical Model for the Determination of Disc edge Vortex Strength, Location and Geometry at Low to Intermediate Flying Speeds", 22nd European Rotorcraft Forum, Brighton (U.K.), September 17-19 1996.

[10] I W Kaynes (DERA), G Preatoni (Agusta), A Visingardi and N Tino (CIRA), C Arzoumanian (Eurocopter), K Kampa (ECD), C. Hermans and B.S.M. Renier (NLR), F Tchen-Fo and N Bettschart (ONERA), R Harrison (GKN-WHL) : "HELIFLOW Pitch-Up and Quartering Flight experiments", 26th European Rotorcraft Forum, The Hague,The Netherlands, September 26-29 2000.

[11] K Kampa, Heliflow Task 2: Quartering Flight. ECD-TN-D/TA2-2000/0005, May 2000.

[12] A Brocklehurst, Analysis of tail rotor performance in low speed quartering flight. GKN-WHL Report RSG/00/0180, March 2000.

[13] Ellin, A.D.S., "An In-*flight Investigation* of. *LYNX AH MK5 Main Rotor/Tail Rotor*. *Interactions*," Proc. 19th European Rotorcraft. Forum, Cemobbio, IT, 1993

[14] E. Hoinville, T. Renaud, CFD simulation of helicopter rotor in the Vortex Ring State regime, 63rd AHS Forum, Virginia Beach, USA 1-3 mai 2007

[15] J. Bailly, A Qualitative Analysis of Vortex Ring State Entry Using a Fully Time Marching Unsteady Wake Model, 36th European Rotorcraft. Forum, 7-9 septembre 2010

[16] Johnson, W., Helicopter Theory, Princeton University Press, 1980.

[17] J. Jimenez. Etude expérimentale et numérique du comportement d'un hélicoptère en descente `a forte pente : modélisation de l'état d'anneaux tourbillonnaires. PhD thesis, Université de la Méditerranée Aix-Marseille II, 2003.

[18] A. Taghizad, J.Jimenez, L.Binet, D.Heuzé, Experimental and theoritical investigation to develop a model of rotor aerodynamics adapted to steep descents, 58th American Helicopter Society Annual Forum, Monréal, Canada, 2002.

[19] Eurocopter - Lettre-Service, No. 1673-67-04 - (clockwise rotation) "Reminder concerning YAW axis control for all helicopters in some flight conditions"

[20] Eurocopter - Lettre-Service, No. 1692-67-04 - (anti-clockwise rotation) "Reminder concerning YAW axis control for all helicopters in some flight conditions"

[21] P.-M. Basset, A. El Omari, "A rotor vortex wake model for helicopter flight mechanics and its application to the prediction of the pitch-up phenomenon", 25th E.R.F., Rome (Italy), paper n°H08, September 1999.


## Copyright Statement